JOURNAL OF MATERIALS SCIENCE 30 (1995) 2163–2170

The environmental effect of SO_2-bearing atmosphere on the creep fatigue failure of aluminide-coated MM-002 nickel-base superalloy at 870 °C

E. AGHION, G. GOVENDER
Department of Mechanical Engineering, University of Natal, King George V Avenue, Durban 4001, South Africa

N. COMINS
Division of Materials Science and Technology, CSIR, Pretoria 0001, South Africa

High-temperature low-cycle fatigue (HTLCF) failure mechanisms of aluminide-coated MAR-M002 nickel-base superalloy in air, argon and Ar + 5% SO_2 atmospheres were investigated at 870 °C. The loading conditions were constant and consisted of creep tension and plastic compression according to the creep plasticity mode of the strain-range partitioning method. The resultant failure mechanisms were investigated using scanning electron microscopy, energy dispersive spectroscopy and X-ray diffraction analysis. The results obtained indicated that the combination of environmental effect and cyclic loading resulted in an early failure of the coating. This failure acted as the incubation and initiation stages for the HTLCF failure of the coated alloy. However, it was found that under an SO_2-containing environment, an accelerated and premature failure was obtained compared to that obtained in argon and air environments. Hence, it is evident that although the aluminide coating provides relatively adequate resistance towards oxidation environment, this protection was ineffective under the SO_2-bearing atmosphere.

1. Introduction

Nickel-base superalloys are used as structural materials in the hot section of jet engines. There are two general types of environmental interaction that result in a reduced service life of these engines, namely oxidation and sulphidation (or hot corrosion if deposits are present) [1]. In order to improve the high-temperature surface stability of these alloys, surface coatings were developed to resist the specific effects of each process.

Although there are several articles on the combination of environmental interaction and fatigue loading [2–5] of nickel-base superalloy, there are few reported studies on the coated alloys. However, the corrosion behaviour of coated nickel-base superalloy has been more extensively studied [6–9]. The general findings in the articles reviewed indicated that aluminide coatings exhibited ample oxidation resistance but were more prone to fail due to sulphidation and hot corrosion. The mechanical properties of high-temperature coatings investigated by Schneider and Grünling [10] indicated that aluminide coatings were fairly brittle, with the number of cycles to first crack under themomechanical fatigue loading being less than ten.

Thus it can be indicated that the mechanism of failure of coated nickel-base superalloy under combination of mechanical loading and environmental interaction is still not completely identified and understood. The aim of the present research was to investigate the influence of Ar + 5% SO_2 environment on aluminide-coated unidirectionally solidified MAR-M002 under a constant high-temperature low-cycle fatigue (HTLCF) loading regime, using air and argon environments as reference atmospheres.

2. Experimental procedure

The material was received as unidirectionally solidified bars of MAR-M002 nickel-base superalloy with the composition shown in Table I. The composition of the material received complied very well with nominal composition of MAR-M002 obtained from Sims *et al.* [11] (Table I). Fatigue specimens were turned from these bars with a gauge length of 25 mm. The diameter of the specimen along the gauge length varied with a minimum diameter of 4 mm at the centre of the gauge length and a maximum diameter of 11.7 mm at the extreme ends of the gauge length.

Additional disc samples were turned in order to evaluate the effect of the environment only. These samples were then chrome aluminide-coated by the packed cementation process. This was followed by ageing at 870 °C for 16 h in an inert environment.

The experimental system used to conduct the HTLCF tests under the controlled atmospheres, described in an earlier paper [2], basically consists of

0022–2461 © *1994 Chapman & Hall*

TABLE I The chemical composition (wt %) of MAR-M002 nickel-base superalloy

	Ni	Cr	Co	W	Ta	Al	Ti	C	Zr	Hf	Others
Material as-received	59.4	8.9	10.4	10.2	1.8	5.2	1.35	0.35	0.23	1.9	0.17 Fe 0.1 Nb
Nominal composition	61	9.0	10.0	10.0	2.5	5.5	1.5	0.14	0.05	1.5	0.015 B

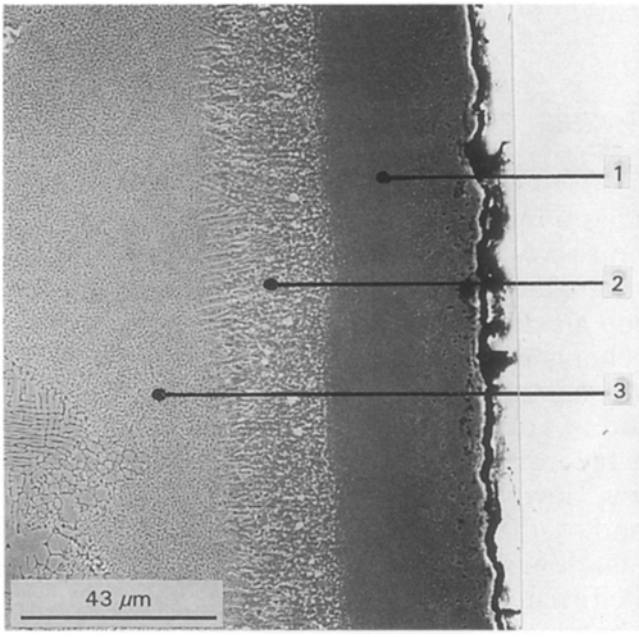

Elements	Layer (Wt %)		
	1	2	3
Al	25.72	9.47	4.76
Ti	-	2.71	1.92
Cr	1.34	9.31	3.26
Fe	0.31	0.37	0.28
Co	7.55	9.56	6.69
Ni	63.45	48.29	67.23
Ta	-	6.22	5.62
W	1.62	11.67	9.90
Hf	-	2.40	-
Nb	-	-	0.33

Figure 1 Microstructure at a longitudinal cross-sectional specimen of coated MAR-M002 with spot chemical analysis of the different layers; etched.

two parts, namely the gas mixing system and thermo-mechanical loading system. The specimen neck was enclosed in a split cylindrical shell through which a specific mixture of gas flowed. The specimen was simultaneously stressed within a split oven furnace via a closed loop servo-hydraulic loading system. The strain across the neck of the fatigue specimen was measured via linear variable displacement transducer (LVDT). Strain transfer rods were attached to the collars on either end of the neck with the LVDT situated outside the furnace. The split cylindrical shell was held together with stainless steel wire and had holes centrally drilled on opposite ends. The controlled gaseous mixture entered through one end while a thermocouple was inserted in the other hole to measure the temperature close to the specimen neck. A positive pressure of approximately 0.5 bar above atmospheric was maintained around the neck to ensure that there was no contamination of the controlled environment.

A constant creep–fatigue loading regime following the strain-range partitioning method was used with creep tension and plastic compression. A constant strain range of $\pm 6.6 \times 10^{-3}$ was used with a tensioning strain rate of $2.6 \times 10^{-4}\,s^{-1}$ and compressive strain rate of $66 \times 10^{-4}\,s^{-1}$. The slow tensioning rate provided the creep component (C) while the high compression rate provided the plastic component (P). The CP loading regime was chosen because creep under tension exerts a significant effect on the failure mechanism in HTLCF.

The HTLCF tests were performed in air, argon and Ar + 5% SO_2 environments with the air and argon atmospheres being used as a reference. The excessive quantity of SO_2 used in the sulphidation environment aimed to amplify the effect of SO_2 in order to obtain an initial clear indication of its effects. In order to determine the influence of the environment only, corrosion tests were performed on unloaded coated and uncoated disc samples in a special corrosion chamber. The specimens were exposed to the various environments (air, Ar, Ar + 5% SO_2) for 5 h at 870 °C. The results were then analysed using scanning electron microscopy (SEM) and X-ray diffraction analyses.

3. Results

The microstructure of unidirectionally solidified MAR-M002 alloy consisted of long dendrites grown in the direction of solidification. The dendritic grain consisted mainly of cuboidal γ' while the interdentritic segregation zone consisted of γ–γ' eutectic phases and some grain-boundary carbides. Metallographic examination of a longitudinal cross-section of a coated sample revealed a typical aluminide coating microstructure, namely the coating layer, interdiffusion zone and substrate (Fig. 1). The coating thickness including the interdiffusion zone was approximately 60 μm. The

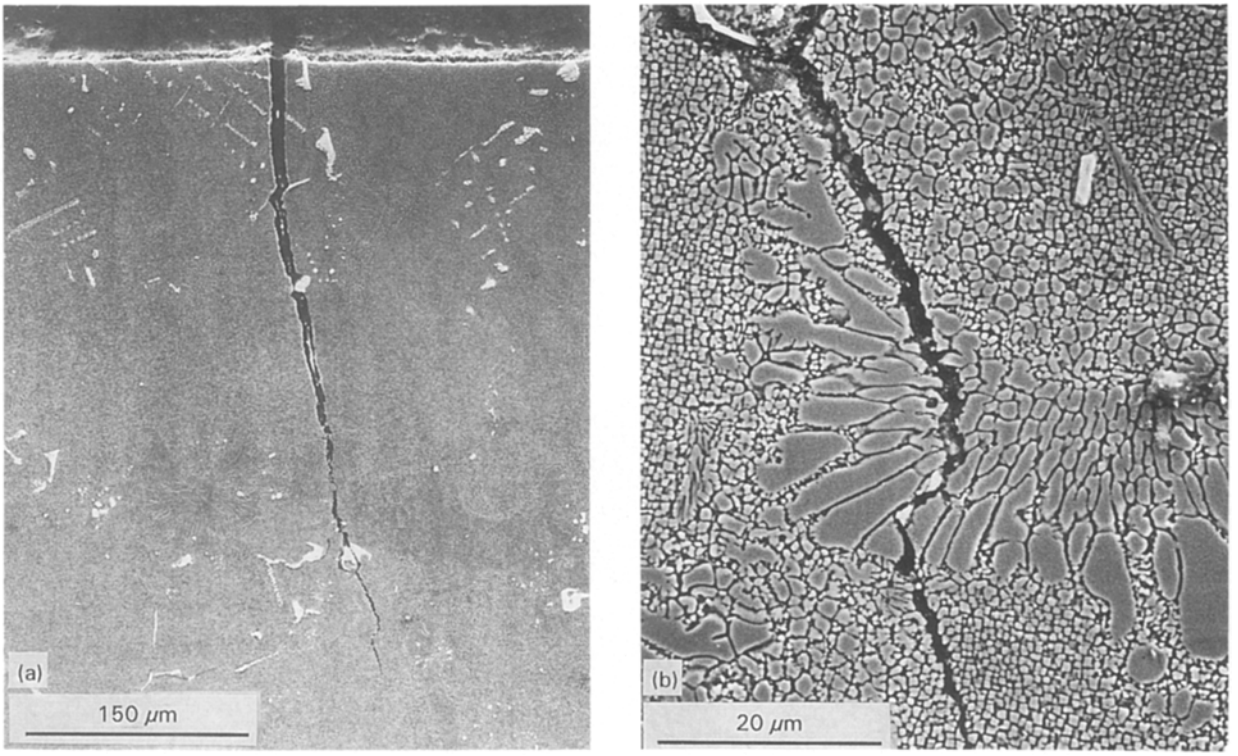

Figure 2 Cross-section of a fatigue specimen after HTLCF failure in an argon atmosphere; (a) a general view, (b) a close-up view of the crack tip.

TABLE II Spot chemical analysis of fatigue crack edge of coated MAR-M002 after HTLCF in argon environment

Examined layer	Ni	Cr	Co	W	Al	Ti	Zr
Close to crack edge	74.29	4.42	9.31	6.56	3.66	1.76	–
Away from crack edge	72.59	5.11	9.30	6.87	3.96	1.50	0.68

chemical analysis of the coating revealed a high weight per cent of aluminium and nickel which are the main constituents of aluminide coatings.

X-ray diffraction analysis of an uncoated disc sample revealed a rich presence of the principal γ'-forming phase, $N_3(Al, Ti)$, as well as Ni_3Ta, Ni_3Hf and some carbides, namely Cr_7C_3 and Cr_3C_2. X-ray diffraction analysis of a coated disc sample disclosed the typical phases present in aluminide coatings, namely NiAl, Al_2O_3, Cr_2O_3 and Cr_3O_4, as well as some of the base metal phases. The NiAl phase is the major constituent of aluminide coatings, while Al_2O_3 and Cr_2O_3 are essentially the protective scales obtained in aluminide coatings.

HTLCF tests performed on several coated specimens at 870 °C in an inert argon atmosphere showed an average life of 877 cycles. Analysis of the fatigue specimen that had failed after HTLCF in argon atmosphere disclosed circumferential cracking of the coating on the external surface close to the fracture surface, which was due to pure mechanical failure of the coating. Metallographic examination of a cross-section close to the fracture indicates that the mode of crack propagation was transdendritic (Fig. 2a). The fatigue crack propagation was relatively "straight" and has initiated from the region where the coating was mechanically cracked. A high magnification of the crack tip (Fig. 2b) shows that there was no evidence of environmental interaction along the crack edge and tip. Chemical analysis along the crack edge (Table II) shows negligible variation in the chemical composition near the crack edge and base material, hence indicating no environmental interaction.

In the air environment, the average HTLCE life of several coated specimens at 870 °C was 670 cycles. Investigation of the fracture surface showed evidence of oxidation (Fig. 3). Circumferential cracking of the coating close to the fracture was evident as in the specimen that had failed in the argon atmosphere. This may indicate that the initial cracking of the coating was due mainly to mechanical loading and not environmental interaction.

Metallographic examination of a cross-section close to the fracture revealed several cracks in the coating (Fig. 4). All cracks were initiated at the cracks in the coating and the mode of propagation was transdendritic. The cracks tended to branch during the propagation stage. Close-up examination of a crack (Fig. 5) revealed porous oxides rich in the reactive elements, such as aluminium and chromium, close to the crack edge. Adjacent to the porous oxide layer is a uniphase layer in which growth and coarsening of the γ' has occurred. The chemical composition of the uniphase layer complies more closely with bulk material with exception of a high concentration of chromium.

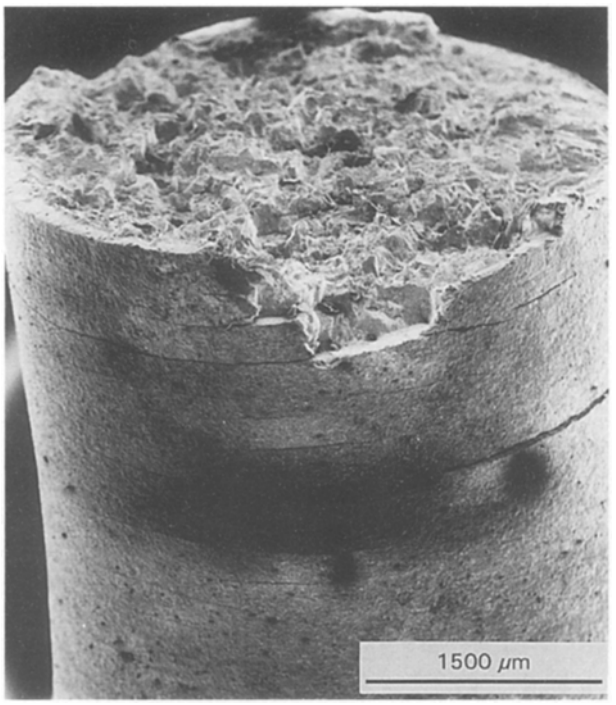

Figure 3 The fracture surface obtained after HTLCF failure in an air atmosphere at 870 °C.

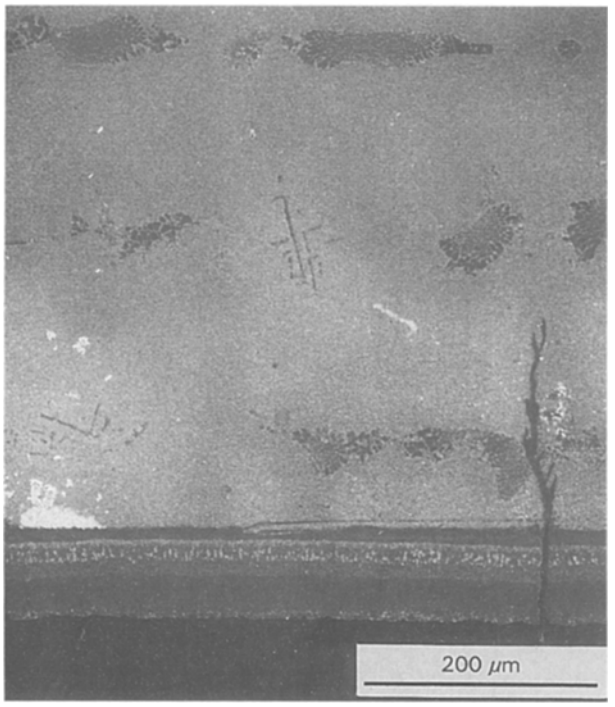

Figure 4 Cracks observed in a longitudinal cross-section after HTLCF in air.

A comprehensive explanation on the nature of the uniphase layer is given in a previous paper [2].

In order to establish performance of the coating in the oxidizing environment, X-ray diffraction analysis was performed on a coated sample exposed to air for 5 h at 870 °C. The X-ray diffraction spectrum shows little variation from the sample as-received, with the exception of additional peaks of Al_2O_3 and $NiCr_2O_4$.

Catastrophic HTLCF failure was observed in the Ar + 5% SO_2 environment with the average number of cycles to failure being less than 50 cycles. The fracture surface was covered with dark sulphide phases (Fig. 6). There were two distinct areas, namely the smooth region where crack propagation occurred and the coarse region where final failure resulted. The concentration of suphide phases was much higher in the smooth region than in the coarse region. This may indicate a severe sulphidation attack in the initial stage of the crack propagation. The average sulphur content on the fracture surface was found to be approximately 5.7 wt %. Circumferential cracking of the coating was observed as in the fatigue specimens that had failed in air and argon atmospheres, thus emphasizing that the fatigue failure under the tested condition was always initiated by the failure of the coating.

Severe sulphidation attack was observed on the coating (Fig. 7) near the fracture surface. Metallographic examination of cross-sectional samples shows extensive damage to the coating (Fig. 8a) and even peeling of the coating near the fracture surface (Fig. 8b). Examination of a crack through the coating indicates that the crack was well developed in the coating but there was some resistance to the sulphidation attack and crack propagation in the interdiffusion zone (Fig. 9). This observation was in agreement with that made by Fryxell and Leese [12] on the role of the interdiffusion zone in hot-corrosion environments of aluminide coatings.

A general view of the longitudinal cross-section of the fracture surface (Fig. 10) showed that the fatigue crack was initiated where the coating was damaged and peeling off. The crack propagation was perpendicular to plane of loading and direction of solidification. The secondary cracks tended to nucleate at the interdendritic segregation zone suggesting that the mode of crack propagation was a mixed trans-interdendritic one. Coalescence and coarsening of the γ' phase was observed adjacent to the fracture surface and secondary crack edges. In order to evaluate the nature of the layers along the crack edge, EDS analysis was performed in the different regions (Fig. 11). A sulphur content of 8.25 wt % was found in the crack manifesting the presence of sulphide phases. There was rich presence of reactive elements aluminium, chromium, and hafnium in the crack indicating the presence of the sulphide phases of these elements and also the oxide phases as a result of the SO_2 breakdown. The presence of sulphur in the second and third layers analysed indicate the penetration of the sulphidation attack.

The X-ray analysis of coated and uncoated transverse cross-sectional disc sample exposed to Ar + 5% SO_2 at 870°C disclose the following results (Fig. 12). For the coated samples (Fig. 12a), there was indication of several sulphide phases present, namely CrS, Ni_3S_2, Al_2S_3 and NiS. The X-ray diffraction spectrum for uncoated MAR-M002 (Fig. 12b) revealed the typical corrosion product that was present along the crack edge, once the coating was penetrated. The sulphide phases present were Ni_3S_4, CrS, Ni_7S_6, NiS and Al_2S_3 as well as Al_2O_3 and NiO phases.

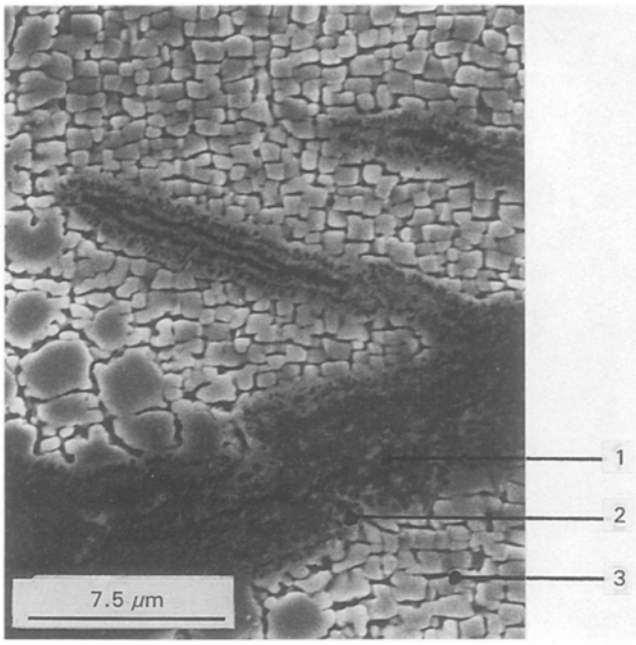

Elements	Layer (Wt %)		
	1	2	3
Al	8.25	8.46	6.47
Ti	2.39	1.74	2.34
Cr	13.84	9.60	3.81
Co	8.14	8.40	6.67
Ni	47.92	56.16	66.37
Zr	3.99	0.52	-
Ta	4.22	3.03	5.38
W	11.25	11.72	8.61
Fe	-	0.37	0.35

Figure 5 Spot chemical analysis of the layers along the crack edge after HTLCF failure in an air atmosphere.

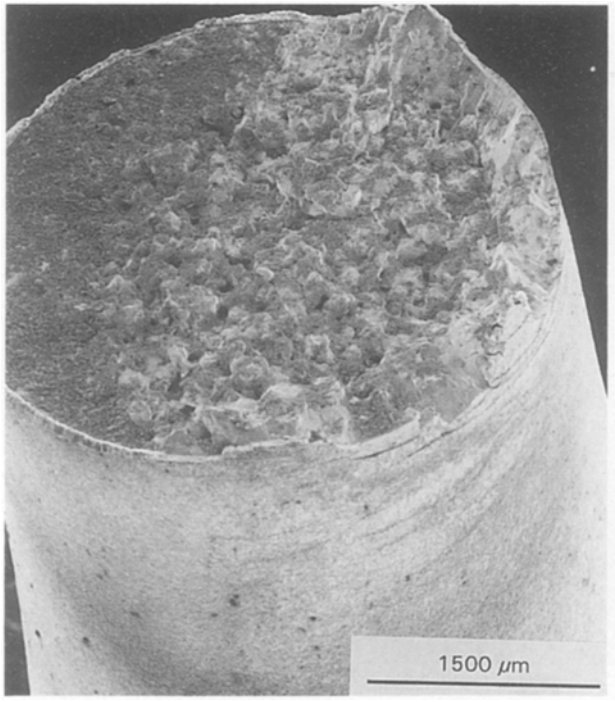

Figure 6 The fracture surface obtained after HTLCF failure in an Ar + 5% SO_2 atmosphere.

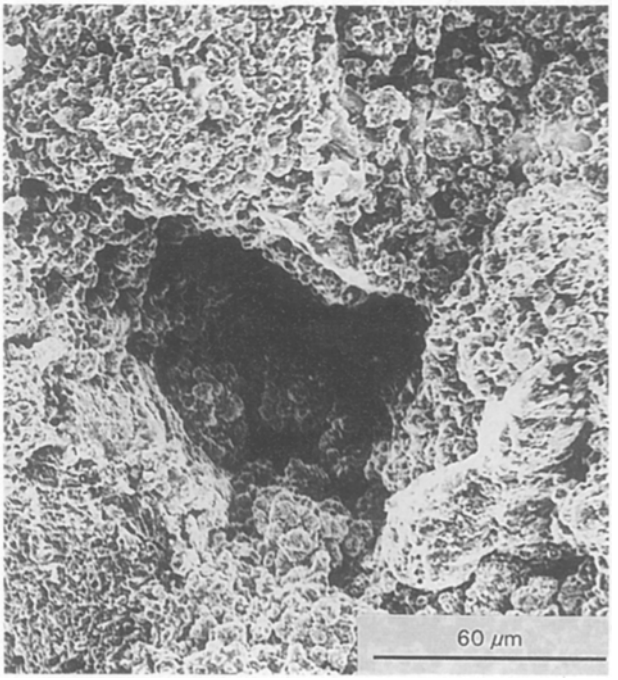

Figure 7 Localized corrosion attack of the coating after HTLCF failure in Ar + 5% SO_2.

4. Discussion

The discussion will focus on the performance of the coating under the combination of environmental interaction and mechanical loading, and the chemical and mechanical events occurring at the region ahead of the propagating crack tip in the unidirectionally solidified alloy under the various environments at 870 °C.

Although cracking of the coating was observed for all the environments tested it was evident that there were significant differences in the nature of crack-growth behaviour within the coating under the various environmental conditions. While the failure in air and argon environments could be considered as mechanically controlled, the failure in the SO_2-containing environment was controlled by the aggressive nature of the environment. This was manifested by the premature failure of the coating in the SO_2 environment accompanied by a severe sulphidation attack which, in some places, causes the coating to peel off completely from the base alloy. In all the tested environments, the cracking through the coating acted as

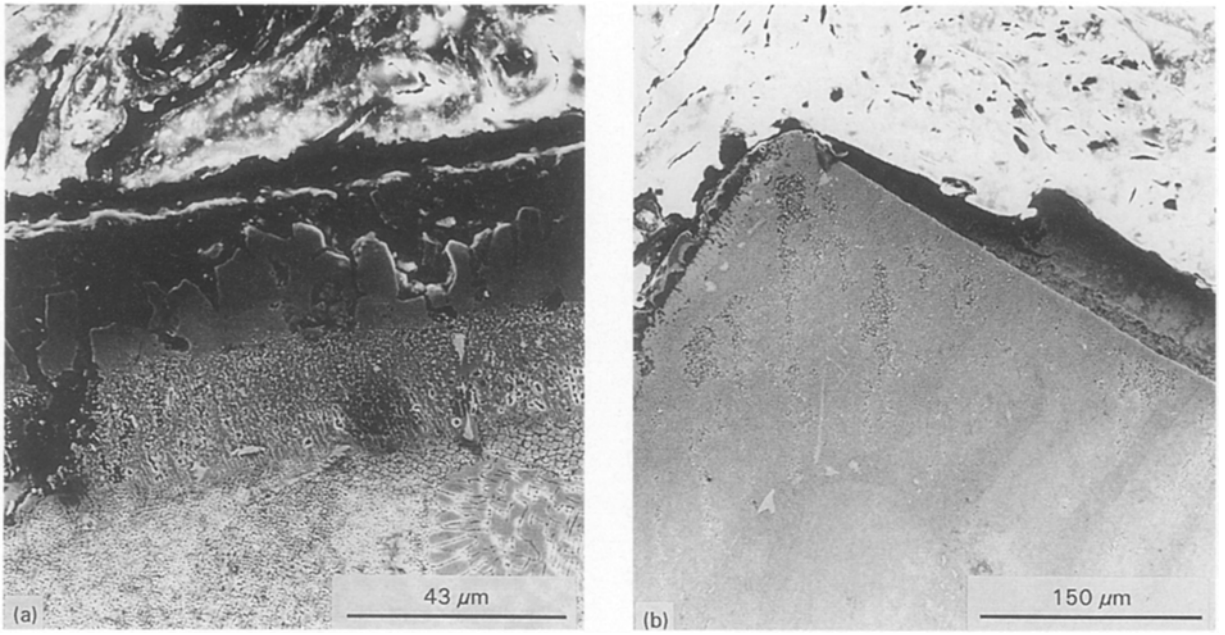

Figure 8 Damage to the coating after HTLCF in Ar + 5% SO_2; (a) general appearance, (b) region where peeling of the coating occurred.

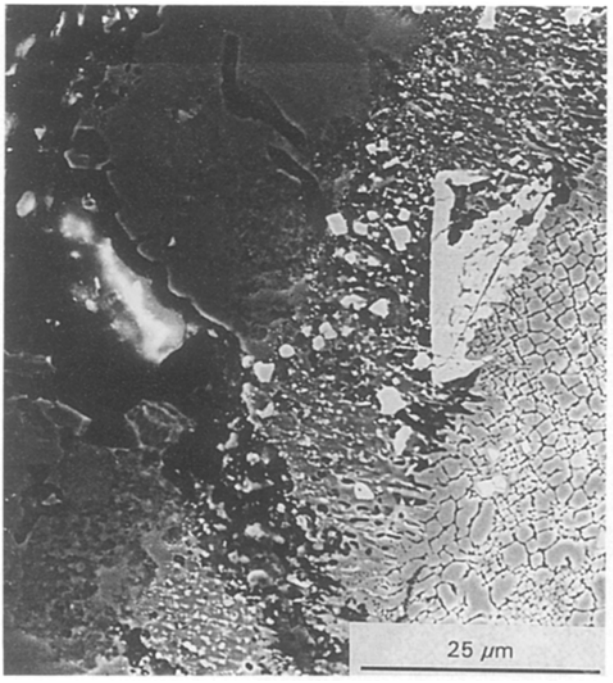

Figure 9 Cracking through the coating after HTLCF in an Ar + 5% SO_2 environment.

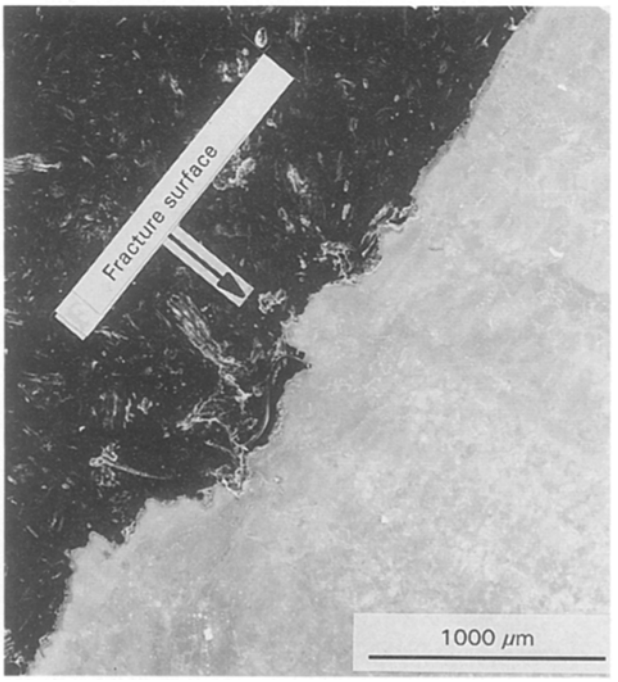

Figure 10 Cross-section showing the intersection between the longitudinal cross-section and fracture surface after HTLCF failure in Ar + 5% SO_2.

the initial stage to the crack propagation in the base alloy.

The failure in the argon atmosphere was marked by the absence of any visible chemical interaction between the substrate and environment. The failure was purely mechanical and the mode of crack propagation was transdendritic. The failure in air atmosphere showed clear indications of environmental interaction with the base material along the propagating crack edge. The crack propagation mode was transdendritic with the crack branching during propagation. The crack edge consisted of three layers, namely the porous oxide layer, the uniphase layer where coarsening or coalescence of the γ' phase occurs and the base metal. The mechanism and formation of the various layers is described in more depth in a previous article [2]. However, the fatigue crack did not show any tendency to initiate and propagate preferentially in the interdendritic zone, as was observed in previous work [2]. This was probably due to the presence of the coating and the role of the coating on the crack propagation behaviour as well as due to the present test conditions, namely lower temperature and difference in the material system and mechanical loading conditions.

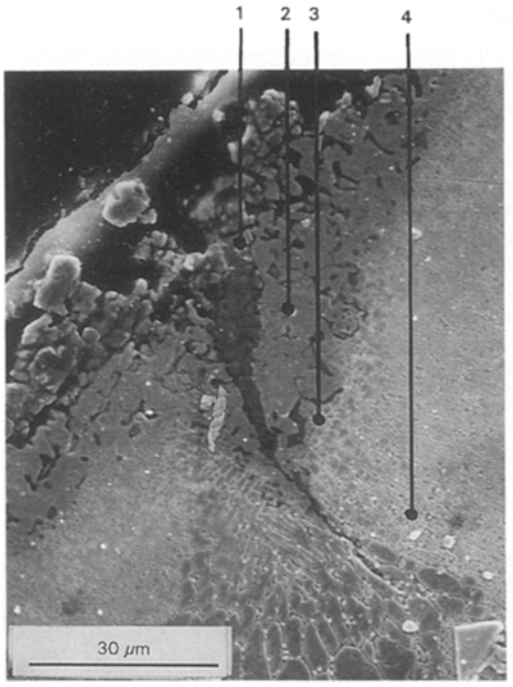

Elements	Layer (Wt %)			
	1	2	3	4
Al	24.35	3.12	3.46	5.89
S	8.25	0.29	0.29	-
Ti	1.17	-	0.91	1.93
Cr	13.27	0.82	3.87	3.49
Co	4.73	12.83	10.70	7.77
Ni	27.86	69.12	71.32	70.81
Zr	-	-	0.77	-
Hf	16.72	-	-	-
Ta	3.66	-	-	1.42
W	-	13.83	8.68	8.69

Figure 11 Spot chemical analysis of the different regions along the crack edge.

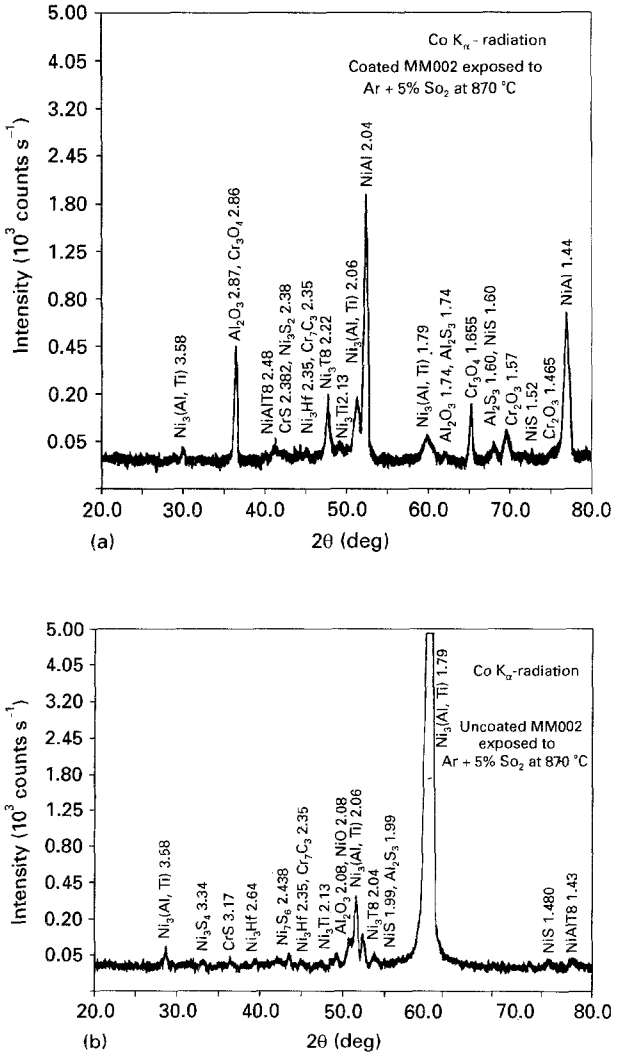

Figure 12 (a) X-ray diffraction of an aluminide-coated disc sample after exposure to Ar + 5% SO_2 at 870 °C. (b) X-ray diffraction analysis of an uncoated disc sample exposed to Ar + 5% SO_2 at 870 °C.

The relatively premature fatigue failure mechanism in the AR + 5% SO_2 environment can be divided into two stages. The first stage is the accelerated failure of the coating which is followed by a second stage of crack propagation through the alloy. At the first stage the coating was severely attacked by the SO_2 environment. As a result of this attack, low-melting sulphide phases such as Ni_3S_2, as well as brittle sulphide phases of the main alloying elements composing the coating, namely Cr_2S_3, CrS and Al_2S_3, were produced. Bearing in mind the brittle nature of the aluminide coating, as was experienced in the failure in air and argon atmospheres, it seems that with the combination of brittle behaviour and extreme sensitivity to sulphidation attack, the premature failure of the coating was inevitable.

As a result of the accelerated failure and cracking of the coating, the second stage, being the crack propagation through the alloy, took place. At this stage the crack-growth behaviour was controlled by the environmental effect of SO_2 ahead of the crack tip. This effect was manifested again by the development of low-melting sulphides which have directly attacked the crack-tip region. In addition to this, one should also consider the formation of brittle sulphide phases, such as CrS and Al_2S_3, as well as oxide phases, such as Al_2O_3 and NiO at the crack tip. These brittle phases will be very prone to crack under the cyclic loading condition, again enhancing the premature failure in the SO_2 environment.

5. Conclusion

Although the tested aluminide coating has provided a relatively reassurable protection under an oxidizing environment in the form of air atmosphere, this was

inadequate under the SO_2-containing environment. The premature fatigue failure of the aluminide-coated superalloy in Ar + 5% SO_2 was due to the aggressive sulphidizing attack of the coating and the region ahead of the propagating crack tip. In all the tested environments, the cracks initiated from the aluminide coating; however, while the failure of the coating in air and argon atmospheres was mainly mechanically controlled, the failure in the SO_2-bearing environment was controlled by the aggressive sulphidizing nature of the environment. Thus, it is quite clear that aluminide coating in its present form could not present an adequate resistance to the combined effect of cyclic loading and SO_2-containing environment, and hence other types of coatings systems, such as platinum aluminide or modified overlay coatings, should be considered for the service conditions in question. We are presently investigating the behaviour of a platinum aluminide coating system under similar conditions. Preliminary results have indicated a superior performance of the platinum aluminide coating compared to the conventional aluminide coating tested.

References

1. E. F. BRADLEY, "Superalloy, a technical guide" (ASM International, Metals Park, OH, 1988).
2. E. AGHION, M. BAMBERGER and A. BERKOVITS, *Mater. Sci.* **26** (1991) 1873.
3. *Idem., Mater. Sci. Eng.* **A147** (1991) 182.
4. E. AGHION, *Mater. Sci. Lett.* **11** (1992) 627.
5. S. FLOREEN and R. H. KANE, *Metall. Trans.* **10A** (1979) 1745.
6. F. S. PETTIT and G. W. GOWARD, "High temperature corrosion and use of coatings for protection", in "Superalloys Source Book" edited by M.J. Donachie, Jr, (American Society for Metals, Metals Park, OH, 1984) pp. 170–85.
7. K. GODLEWSKI and E. GODLESKA, *Mater. Sci. Eng.* **88** (1987) 103.
8. T. N. RHYS-JONES and N. SWINDELLS, *Corr. Sci.* **25** (1985) 559.
9. K. NATESAN, *Mat. Sci. Eng.* **87** (1987) 99.
10. K. SCHNEIDER and H. W. GRÜNLING, *Thin Solid Films* **107** (1983) 395.
11. C. T. SIMS, N. S. STOLOFF and W. C. HAGEL, "Superalloys II" (Wiley, New York, 1987).
12. R. E. FRYXELL and G. E. LEESE, *Surf. Coat. Technol.* **32** (1-4) (1987) 97.

Received 30 March 1993
and accepted 5 September 1994